Energy & Environmental Science

Accepted Manuscript

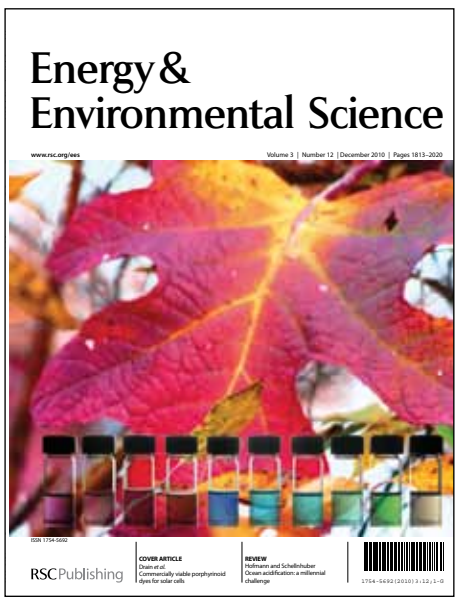

This is an *Accepted Manuscript*, which has been through the RSC Publishing peer review process and has been accepted for publication.

Accepted Manuscripts are published online shortly after acceptance, which is prior to technical editing, formatting and proof reading. This free service from RSC Publishing allows authors to make their results available to the community, in citable form, before publication of the edited article. This *Accepted Manuscript* will be replaced by the edited and formatted *Advance Article* as soon as this is available.

To cite this manuscript please use its permanent Digital Object Identifier (DOI®), which is identical for all formats of publication.

More information about *Accepted Manuscripts* can be found in the **Information for Authors**.

Please note that technical editing may introduce minor changes to the text and/or graphics contained in the manuscript submitted by the author(s) which may alter content, and that the standard **Terms & Conditions** and the **ethical guidelines** that apply to the journal are still applicable. In no event shall the RSC be held responsible for any errors or omissions in these *Accepted Manuscript* manuscripts or any consequences arising from the use of any information contained in them.

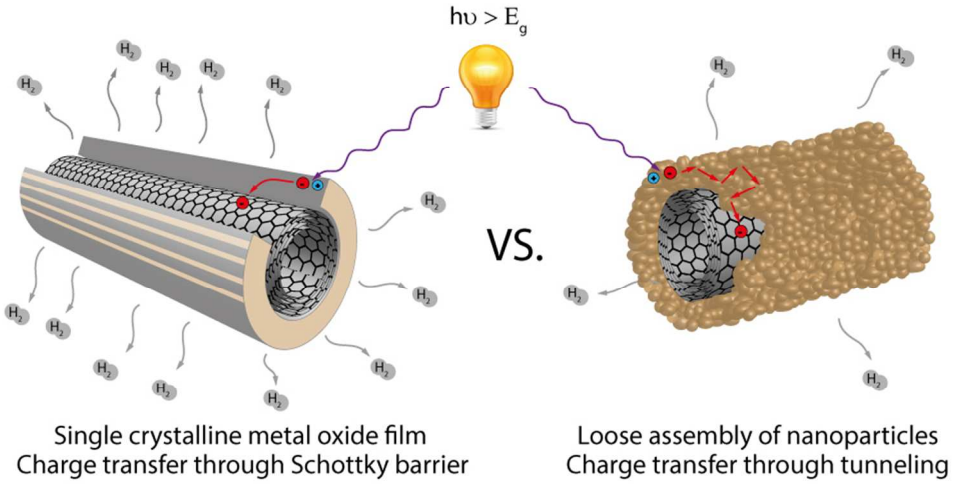

254x126mm (100 x 100 DPI)

Cite this: DOI: 10.1039/c0xx00000x

www.rsc.org/xxxxxx

ARTICLE TYPE

Interface Engineering In Nanocarbon-Ta_2O_5 Hybrid Photocatalysts

Alexey S. Cherevan,[a] Paul Gebhardt,[a] Cameron. J. Shearer,[a] Michinori Matsukawa,[b] Kazunari Domen,[b] Dominik Eder[a]*

Received (in XXX, XXX) Xth XXXXXXXXX 20XX, Accepted Xth XXXXXXXXX 20XX

DOI: 10.1039/b000000x

Hybridizing inorganic nanomaterials with carbon nanotubes and graphene constitutes a powerful approach towards creating new functional materials for environmental and sustainable energy applications. Their superior performance originates from synergistic effects based on charge and energy transfer processes at the hybrid's interfaces. However, only few works have been devoted so far towards rationally designing these hybrids. In this work we demonstrate that engineering interfaces as well as the morphology of the functional inorganic compound can maximise the synergistic effects in hybrids, thus further enhancing the hybrid's photocatalytic properties. Particularly, we have stimulated the growth of ultra-thin single-crystalline layers of tantalum (V) oxide (Ta_2O_5) with preferred orientation at substantially reduced crystallisation temperatures, by utilising the graphitic CNTs surface as seed crystals through heterogeneous nucleation. The resulting hybrids possess outstanding activities for the evolution of hydrogen via sacrificial water splitting that are about 35 times higher than comparable materials such as tantalates. The additional improvements in this hybrid are attributed to the single-crystalline nature of the coating, which alleviates transport of electrons to the interface, as well as the formation of a Schottky-type junction between the metallic nanocarbon and the semiconducting metal oxide, which facilitates charge transfer and thus charge separation at the interface.

Cite this: DOI: 10.1039/c0xx00000x

www.rsc.org/xxxxxx

ARTICLE TYPE

Introduction

There is an ever growing need to protect our natural environment by increasing the achievable energy efficiency and invention of sustainable "green" energy sources. Notably, exploitation of the sunlight's energy to split water into its constituent elements, oxygen and hydrogen, constitutes the key requirement to successfully establish hydrogen gas as a clean energy source and was recently identified by the European Science Foundation as one of the world's emerging key research fields. Many conventional materials in photocatalysis (i.e. chalcogenides, ceramics) cannot fulfil all requirements for these new technologies, but in addition to the development of new materials, careful optimization of suitable material combinations that may benefit from synergistic functions can be considered as viable approach to functional compounds.

The hybridization of rather cheap and non-toxic semiconductors, such as metal oxides and (oxy)nitrides, with abundant carbon species including graphene or carbon nanotubes (CNTs), provides a powerful strategy to rationally design new multifunctional materials.[1] Notably, the nanocarbon's ability to absorb photons, accept and conduct electrons, and exchange phonons with the inorganic compound renders such hybrids suitable as promising candidates for a variety of applications like photocatalysis, chemical sensing, batteries, supercapacitors, field emission devices, and photovoltaics.[1-4]

Indeed, early studies have documented considerable improvements in the photocatalytic performance of hybrids over their individual constituents, mostly concentrating on the degradation of organic compounds.[5-9] As an example, the activity of the zeolite TS-1 for the oxidation of 4-nitrophenol increased by a factor of 5-6 upon hybridization with just a few weight percent of CNTs or graphene.[10, 11] These remarkable enhancements are generally attributed to two effects: a photosensitization effect of the nanocarbon, which slightly extends absorption into the visible range[12, 13], and interfacial charge and energy transfer processes, which facilitate electron-hole separation, so leading to longer lifetimes of the charge carriers.[2, 12-14]

Photocatalytic water splitting is yet another, highly promising application, which has been gaining tremendous interest following its discovery in 1972 has as a promising route towards producing clear energy using sun-light.[15-17] Surprisingly, only few studies have so far investigated the potential of nanocarbon hybrids for this application, typically using TiO_2, CdS and g-C_3N_4 as the semiconducting photocatalyst and only reporting modest enhancements in the range of 2-3 times.[18-24]

In this work, we demonstrate that the photocatalytic properties of nanocarbon hybrids for sacrificial water splitting can be further enhanced considerably over simple surface coupling by purposefully engineering interfaces and the morphology of the hybrids. Particularly, we hybridized both multi-walled CNTs and graphene oxide (GO) with Ta_2O_5, which is a cheap and non-toxic semiconductor, yet with a comparatively large band gap of ~ 3.9 eV.[25] Although most of contemporary research on photocatalytic water splitting concentrates on visible-light active materials, Ta_2O_5 can offer a simple model system for hybridization studies that can in future be extended to other tantalum oxide based semiconductors, some of which are presently among the most active photocatalysts for water splitting, i.e. $NaTaO_3$,[26-28] $LiTaO_3$,[29] TaON[30] and Ta_3N_5.[31, 32] We want to emphasize that this tool of interface engineering can also be utilised to improve the performance of nanocarbon hybrids in other applications, such as photovoltaics, sensors and energy storage devices.

Results and disscussion

We used multi-walled carbon nanotubes (CNT) grown via a continuous-flow chemical vapour deposition technique (CVD) using ferrocene as the catalyst precursor and toluene as carbon feed. The CNTs were subsequently purified in argon at 1000 °C.[33] Graphene oxide (GO) with predominantly 1-3 layers was produced via chemical exfoliation of graphite following a modified Hummer's route.[34] The nanocarbons were hybridized in-situ via a hydrothermally-assisted sol-gel route using $Ta(OEt)_5$ as precursor. Two CNT to metal oxide weight ratios, 1:4 and 1:2, were chosen to produce hybrids with thick and thin Ta_2O_5 coatings, denoted H1 and H2, respectively. The samples were subsequently annealed in nitrogen at 500 °C and 700 °C, the latter being the typical crystallization temperature of bulk Ta_2O_5.[35]

Scanning electron microscopy (SEM, Fig S1†), transmission electron microscopy (TEM, Fig. 1) and UV-Vis absorption spectroscopy (Fig. S2A†) confirm that the nanocarbons were successfully hybridised with tantalum oxide. In case of the GO-Ta_2O_5 hybrids, the functional groups of GO facilitated the adsorption of very small Ta_2O_5 particles (5-10 nm), which were well distributed over the entire carbon surface (Fig. S1C†). In contrast, the deposition of Ta_2O_5 onto CNTs was more challenging, due to the hydrophobic nature of highly crystalline multi-walled CNTs after pretreatment in argon at 1000 °C. Most commonly, the CNTs are functionalized covalently, i.e. by oxidative acid treatment, which renders the surface hydrophilic, yet typically results in a random distribution of functional groups and also disrupts the aromatic nature and thus the properties of the outer carbon layer.[1] In the present work we opted for a non-destructive modification, using benzyl alcohol (BA) as a linking agent, which we have recently developed for the coating of CNTs with TiO_2.[36] In short, the BA molecules adsorb on the entire CNT surface via π-π interactions thereby providing rather uniformly distributed hydroxyl groups for the attachment of the hydrophilic precursor molecules.[37] SEM indeed confirmed the presence of a conformal Ta_2O_5 coating covering the entire surface of the BA-modified CNTs, while containing only few fractures due to the drying process. The thickness of the coating was very uniform

and dependent on the initial CNT-to-metal oxide ratio (Fig. S1A,B†).

The photocatalytic performance of these samples was tested for hydrogen evolution through sacrificial water splitting. Due to the rather large band-gap of Ta_2O_5 of 3.9 eV, the samples were irradiated with UV light using a high pressure Hg lamp.

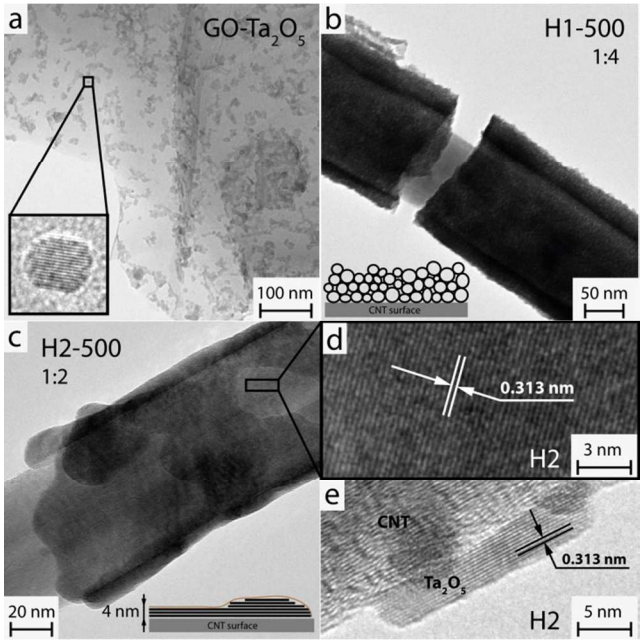

Fig. 1 HRTEM image of GO-Ta_2O_5 hybrid consisting of well distributed crystalline oxide particles on the GO surface (A). TEM images of CNTs:Ta_2O_5 hybrid with morphology types H1 (B) and H2 (C) corresponding to thick and thin coatings, respectively. Insets schematically represent the corresponding coating morphology. HRTEM images of the H2-500 hybrid showing (101) lattice fringes of the Ta_2O_5 layer (D) and the tight interface between CNTs and Ta_2O_5 (E).

The experiments were conducted in a closed gas circulation system, each using 50 mg of the photocatalyst, and the evolved gasses were analysed via gas chromatography (more details in Methods). Platinum was chosen as a co-catalyst to aid desorption of molecular hydrogen. The photocatalysts were loaded with 0.5 wt.% Pt via in-situ photodeposition,[38] which yielded uniformly sized (2.7 ± 0.3 nm) nanoparticles that were well dispersed over the entire hybrid surface (HRTEM data, Fig. 2A). The amount of hydrogen produced intrinsically via UV-assisted methanol oxidation on Pt (i.e. through C=O excitation) was quantified for uncoated CNTs, which were loaded with the same amount of Pt, and subsequently subtracted from the measured rates for the photocatalysts. Furthermore, we designed a new reference material in order to eliminate any effect of specific surface area on the photocatalytic activity. Ta_2O_5 nanotubes (Ta_2O_5-NT) were synthesized for the first time by calcining the hybrids in air at 600°C to remove the CNT template, following previous studies on TiO_2 nanotubes.[39] SEM, EDX and XRD (absence of the 002 diffraction at $2\theta = 26.5$ °) confirmed that carbon was completely removed and that the tubular morphology was preserved (Fig. S1D† and Fig. 3A). BET revealed a similar specific surface area (35 m^2/g) as the hybrids (27-32 m^2/g). The activity for these reference nanotubes was measured to be 45 $\mu molh^{-1}$. Similar values using a comparable experimental setup (i.e. light source, reactor design) were reported for various titanates,[40] tantalates[41] and niobates.[42] The slightly higher activity in our nanotubes may well be attributed to its nanotubular morphology and thus its larger surface area.

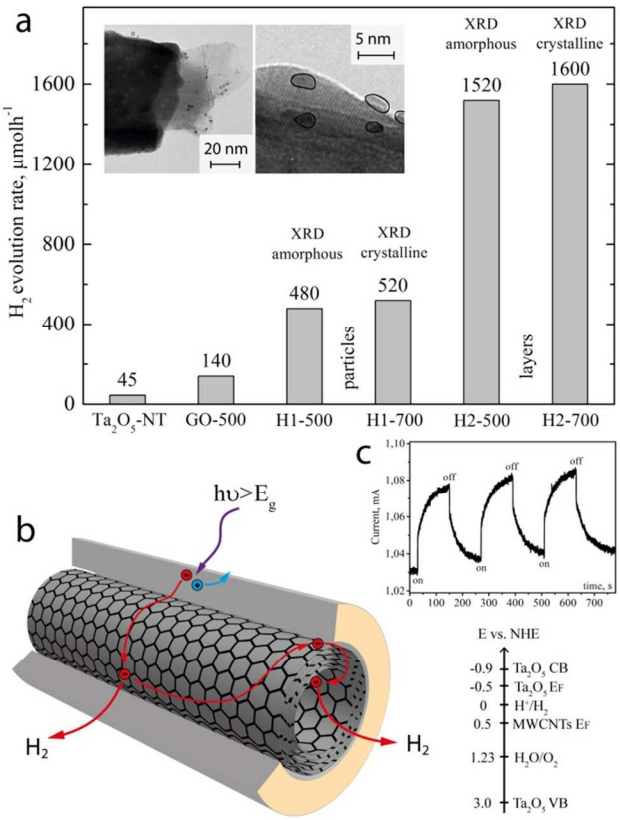

Fig. 2 Hydrogen evolution rates in water splitting for 50 mg of a photocatalyst loaded with Pt cocatalyst for Ta_2O_5 nanotubes, GO-Ta_2O_5 hybrid treated at 500 °C and H1 and H2 type hybrids treated at 500 °C and 700 °C and inset demonstrating photodeposited Pt nanoparticles on the hybrid surface (A). Proposed mechanism of electron-hole transfer in the CNT-Ta_2O_5 hybrids and the associated energy levels diagram containing energy band and Fermi level positions of Ta_2O_5, Fermi level of MWCNTs and red/ox potentials of water (B). I-t response curves of CNTs-Ta_2O_5 with an external bias of 0,01 V under UV illumination (on) and dark (off) demonstrating the photoresponse of the hybrid (C).

The respective rates for all photocatalysts are summarized in Fig. 2A. The hybridization of Ta_2O_5 with GO and CNTs has indeed improved the activity remarkably. For example, GO enhanced the activity of Ta_2O_5 by a factor of approx. 3 (140 $\mu molh^{-1}$ for GO-500), which is a similar improvement over the pure component as reported for GO-TiO_2 hybrids.[16, 17, 40, 41] Most notably, hybridization with CNTs has resulted in considerably greater enhancements than with GO, which is in contrast to most literature reports.[3, 13, 21] Considering that the amount of Ta_2O_5 in the GO hybrid (ca. 20 %) was lower than in the CNTs hybrids (65 and 80 % for H1 and H2, respectively), it is possible that GO- Ta_2O_5 can be further optimized by increasing the metal oxide content. In addition to this, annealed CNTs are expected to possess better charge transfer properties than highly defective graphene, but nevertheless the difference in activity by one order of magnitude between the GO and CNT hybrids is remarkable and justifies further investigations.

The most striking feature is that the H2 hybrids (up to 1600 μmolh^{-1} for H2-700) exhibited a 3-4 times higher activity than the H1 hybrids (up to 520 μmolh^{-1} for H1-700). In fact, the H2 hybrid was considerably more active than Pt loaded TiO_2-P25 (700 μmolh^{-1}) and, more impressively, 35 times more active than the Ta_2O_5-NT and thus other tantalates in literature,[41] thus reflecting unprecedented large activities for UV-based photocatalysts. Remarkably, there was no significant difference (less than 10 %) for hybrids treated at either 500 °C or 700 °C, which is rather surprising considering that Ta_2O_5 typically requires temperatures well above 670 °C for crystallization.

This outstanding enhancement of photocatalytic performances in Ta_2O_5 containing hybrids can be attributed to several effects: a major contribution stems from interfacial charge transfer processes, created through hybridization of Ta_2O_5 with GO and CNTs, which can affect the performance in two different ways: a) nanocarbons can act as photosensitizers though extending the absorption range and delivering additional electrons to the valence band (VB) of the metal oxide;[12, 13] and b) nanocarbons can act as electron acceptors for photoexcited electrons from the conduction band (CB) of the metal oxide, thus reducing electron-hole pair recombination and increasing the exciton lifetime.[14] Fig. 2B illustrates the electron-hole transfer mechanism in the CNTs-Ta_2O_5 hybrids and shows the energy diagram for the CNTs-Ta_2O_5 system with respect to the water redox potentials and reveals that the Fermi level of multi-walled CNTs lies well below the Fermi level of the metal oxide.[25] In order to confirm interfacial charge transfer in our CNT hybrids, we have measured the photoresistive response of our hybrids while applying a bias of 0.01V. The chronoamperometric data in Fig. 2C show that the photocurrent increased considerably under irradiation due to increased numbers of charge carriers. This confirms that photoexcited electrons are transferred from the Ta_2O_5 through the interface into the CNTs in line with the aforementioned energy diagrams.

Interfacial charge transfer processes have been solely accounted for the modest enhancements in nanocarbon hybrids reported so far.[1, 2] The more pronounced enhancements in our CNT hybrids may stem from the comparatively small particle size of Ta_2O_5, which was less than 4 nm (Fig. 1). Indeed, the UV-Vis absorption spectrum in Fig. 3D reveals a significant blue-shift of the absorption edge, resulting in a band gap of ~ 4.0 eV that is about 0.1 eV larger than pure Ta_2O_5. A larger band gap corresponds to a higher conduction band level, thus to a higher energy of the photoexcited electrons, which consequently increases the probability of successful H^+ reduction.[43]

These contributions, however, do not solely explain the remarkably higher activities for the H2 over the H1 hybrids. Contributions of the specific surface area can be neglected, since BET provided similar surface areas of 27 and 32 m^2/g, for H1 and H2, respectively. In fact, this slight increase in surface area can possibly account for only 18 % increase in activity. It is evident that the disparity in performance between H1 and H2 is linked to the morphology of their coatings, which was remarkably different between the two hybrids. In case of H1, the coating consisted of several layers of loosely aggregated nanoparticles (Fig. 1B). The size of the particles was remarkably small and increased only slightly with annealing temperature from 3-4 nm at 500 °C (H1-500) to 4-6 nm when heated at 700 °C (H1-700). A similar morphology, yet typically with significantly larger particles, has generally been observed for nanocarbon hybrids with TiO_2[39] and other metal oxides.[44] In contrast, the coating in the H2 hybrids resembled an amorphous thin film covering a surface area several hundreds of nanometres across (Fig. 1C). A closer look by TEM revealed that the film consisted predominantly of a single layer, whose thickness increased from 3-4 nm at 500 °C to 6-8 nm at 700 °C. Occasionally, a second layer with few grain boundaries, resembling the shape of platelets, was found on top of the first layer.

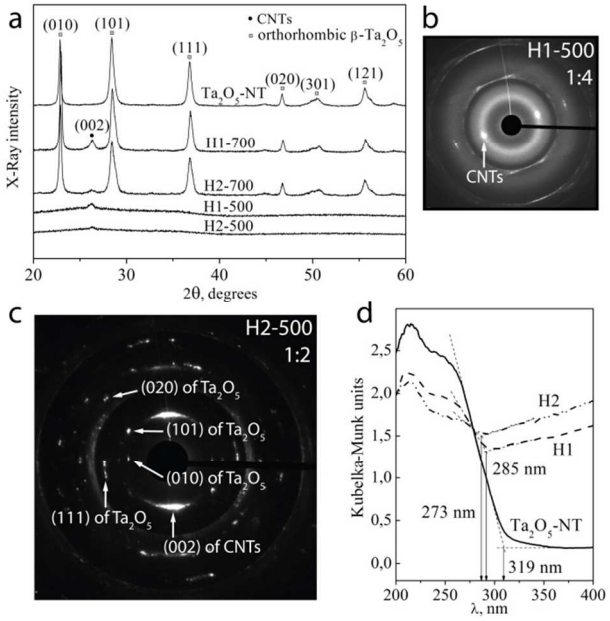

Fig. 3 XRD diffractograms of the CNTs-Ta_2O_5 hybrids annealed at different temperatures as well as of reference Ta_2O_5 nanotubes (A). ED patterns of the H1-500 hybrid containing only (002) diffraction of CNTs (B) and H2-500 hybrid indicating a single crystalline nature of the oxide coating (C). UV-VIS-reflectance spectra of H1 and H2 morphology type CNTs-Ta2O5 hybrid as well as of reference Ta_2O_5 nanotubes (D).

X-ray diffraction (XRD, Fig. 3A) confirmed that the hybrids treated at 700 °C contained a crystalline coating consisting of orthorhombic β-Ta_2O_5 phase.[45] Further refinement of the XRD data provided a unit cell with the dimensions a = 6.214 Å, b = 3.878 Å and c = 3.636 Å. The hybrids annealed at 500 °C showed no reflexes apart from a weak peak at 2θ = 26.4 °, which corresponds to the (002) spacing in multi-walled CNTs (Fig. S2B†). The absence of any diffraction corresponding to Ta_2O_5 indicates that the Ta_2O_5 coating was either amorphous or consisted of crystals too small to be detected by XRD (i.e. < 4 nm). Therefore, we used the more sensitive electron diffraction (ED) to analyse the hybrids treated at 500 °C in more detail. The ED image of H1-500 showed only the (002) diffraction from the CNTs and no additional features, i.e. fine rings, that could be assigned to nanocrystalline Ta_2O_5 (Fig. 3B). In contrast, the pattern of H2-500 sometimes contained strong individual diffraction spots at positions expected from orthorhombic β-Ta_2O_5 (Fig. 3C), indicating that some areas of the coating were crystalline, even at temperatures well below 500 °C.

In addition, the appearance of just a few, individual spots rather than diffuse halos further suggest the presence of single crystals. A closer look with HRTEM indeed confirmed the single-crystalline nature of the Ta_2O_5 film in H2-500 °C and further revealed a preferential growth with respect to the CNT surface (Fig. 1D). The observed fringes of the Ta_2O_5 film correspond to the (101) and (111) spacing of β-Ta_2O_5 phase (0.313 nm and 0.244 nm, respectively), in line with literature data.[45]

The combined results suggest that the H1 hybrid contains a particulate coating with polycrystalline nanoparticles at 700 °C. The size of the Ta_2O_5 nanoparticles is considerably smaller than that of Ta_2O_5 produced without CNTs following identical synthesis conditions (> 100 nm), indicating an active role of CNTs in the crystal growth. Recently, we have demonstrated that CNTs can act as a "heat sink" thereby dissipating excess heat during the crystallization of TiO_2 particles, thus hindering their growth.[39] A similar effect may be responsible for very small Ta_2O_5 particles in the H1 hybrid.

The situation for the H2 hybrids is entirely different, as part of the Ta_2O_5 film was already crystalline at 500 °C, which is about 200 °C lower than typically required for pure Ta_2O_5. At such low temperatures, the crystallization of Ta_2O_5 is kinetically limited by the activation energy rather than thermodynamically by the Gibbs energy. The considerably reduced crystallization temperature in H2 is thus related to the lower activation energy for heterogeneous nucleation than homogeneous nucleation, which suggests a favourable interaction between the two compounds. The major synthetic difference between the two hybrids H1 and H2 is the CNT to Ta_2O_5 weight ratio, which is expressed by the different thickness of the coating. It is likely, that the crystallization in H1 proceeds via 3D homogeneous nucleation, leading to the formation of small Ta_2O_5 particles, while heterogeneous nucleation becomes dominant at low concentrations such as in H2, i.e. initiated by structural defects in CNTs acting as seed crystals.[46] If structural defects at CNT surfaces constitute active sites for nucleation, their number will affect the size of the crystals. The defect concentration in our annealed CNTs is very low, as indicated by the low D/G ratio in Raman spectroscopy (Fig. S2C†), hence is accounting for the large single-crystals that extend over several hundreds of nanometres across

In view of the detailed understanding of the structure and morphology of our hybrids, we can now attribute the enhanced performance of H2 over H1 to several additional effects. First, the number of grain boundaries in the H2 hybrid is considerably reduced over that in H1 due the more single-crystalline nature of H2. Grain boundaries are known as centres for charge recombination.[17] Consequently, fewer grain boundaries along with shorter diffusion lengths in the thin Ta_2O_5 layers increase the probability of successful charge transport to the interface. Second, the nature of the interface affects the efficiency of charge separation. In contrast to the loose aggregation of Ta_2O_5 particles in H1, in which the absence of direct electronic contacts requires charge transfer via tunnelling over a long distance, the growth of Ta_2O_5 in H2 forms a tight Schottky-type junction between the semiconductor and the MWCNT, which is considered metallic conductor due to the graphite-like interactions between the individual walls. Such a junction would reduce the barrier for charge transfer considerably and thus enhances the charge separation through electron extraction by CNTs (Fig. 1E). Finally, the difference in activity may be a consequence of an altered band structure of Ta_2O_5 in H2 due to band interactions between CNTs and Ta_2O_5. This is supported by UV-Vis spectroscopy (Fig. 3D), which revealed that the absorption band of Ta_2O_5 in H2 is blue-shifted from 285 nm to 273 nm, thus increasing the band-gap by a further 0.19 eV compared to H1. A larger band gap would correspond to an increased reduction potential of the photoexcited electrons, which in turn could enhance the photocatalytic activity for water reduction.[43]

We also measured the long term stability of our CNTs-Ta_2O_5 hybrids. Remarkably, the activity of hydrogen evolution remained constant even after 20 h of UV exposure as can be seen in Fig. S2D†. These results indicate that CNTs have improved both performance and stability of the photocatalyst.

Conclusions

In summary, we demonstrated that the photocatalytic properties of nanocarbon hybrids can be further improved by purposefully engineering the interfaces and morphology of the active layer. In contrast to the typical attachment of loose aggregates of metal oxide particles on CNTs, we have grown ultra-thin single-crystalline Ta_2O_5 films by utilising the graphitic CNT surface as seed crystals for heterogeneous nucleation. The resulting hybrids exhibited very high activities and stability for sacrificial water splitting. In addition to synergistic effects offered by nanocarbon-inorganic hybrids, the further improvements in our hybrid are attributed to the single-crystalline nature of the coating, which alleviates transport of electrons to the interface, as well as the formation of a Schottky-type junction between the overall metallic CNTs and the semiconducting metal oxide, which facilitates charge transfer (as confirmed by photoresistance measurements) and thus charge separation at the interface. Our approach can be extended to e.g. visible light driven photocatalysts and constitutes a general opportunity for nanoscaled engineering of nanocarbon hybrids suitable for other energy conversion and storage applications. Considering the superior performance of our hybrids with CNTs over those with graphene oxide, we further recommend to compare different types of nanocarbons for a specific application.

Acknowledgements

We acknowledge the funding by the European Union's 7th Framework Program FP7/2007-2013 under grant agreement n° 310184. A.C. is grateful for financial support by the Graduate School of Chemistry at the University of Münster. M.M. and K.D. would like to thank the Grant-in-Aid for Specially Promoted Research (no. 23000009) of the Japan Society for the Promotion of Science (JSPS). We further thank Prof. G. Brunklaus (Münster), Prof. U. Steiner (Cambridge) and Prof. B. Klötzer (Innsbruck) for fruitful discussion and H. Hu (Münster) for providing the graphene oxide.

Notes and references

[a] *Institute of Physical Chemistry, Westfälische Wilhelms-Universität*

Corrensstrasse 28/30, Münster, 48149, Germany. E-mail: dominik.eder@uni-muenster.de.
[b] Department of Chemical System Engineering, The University of Tokyo 7-3-1 Hongo, Bunkyo-ku, Tokyo 113-8656, Japan

† Electronic Supplementary Information (ESI) available: medhods, SEM images, UV-Vis, Raman and ED characterisation. See DOI: 10.1039/b000000x/

1. D. Eder, *Chemical Reviews*, 2010, **110**, 1348-1385.
2. J. J. Vilatela and D. Eder, *ChemSusChem*, 2012, **5**, 456-478.
3. L. Ge and C. Han, *Applied Catalysis B: Environmental*, 2012, **117–118**, 268-274.
4. Q. Xiang, J. Yu and M. Jaroniec, *The Journal of Physical Chemistry C*, 2011, **115**, 7355-7363.
5. B. Liu, Y. Huang, Y. Wen, L. Du, W. Zeng, Y. Shi, F. Zhang, G. Zhu, X. Xu and Y. Wang, *Journal of Materials Chemistry*, 2012, **22**, 7484-7491.
6. N. Bouazza, M. Ouzzine, M. A. Lillo-Ródenas, D. Eder and A. Linares-Solano, *Applied Catalysis B: Environmental*, 2009, **92**, 377-383.
7. J. Du, X. Lai, N. Yang, J. Zhai, D. Kisailus, F. Su, D. Wang and L. Jiang, *ACS Nano*, 2010, **5**, 590-596.
8. T. Lv, L. Pan, X. Liu and Z. Sun, *Catalysis Science & Technology*, 2012, **2**, 2297-2301.
9. N. Zhang, Y. Zhang, M.-Q. Yang, Z.-R. Tang and Y.-J. Xu, *Journal of Catalysis*, 2013, **299**, 210-221.
10. M. Krissanasaeranee, S. Wongkasemjit, A. K. Cheetham and D. Eder, *Chemical Physics Letters*, 2010, **496**, 133-138.
11. Z. Ren, E. Kim, S. W. Pattinson, K. S. Subrahmanyam, C. N. R. Rao, A. K. Cheetham and D. Eder, *Chemical Science*, 2012, **3**, 209-216.
12. W. Wang, P. Serp, P. Kalck and J. L. Faria, *Journal of Molecular Catalysis A: Chemical*, 2005, **235**, 194-199.
13. H. Zhang, X. Lv, Y. Li, Y. Wang and J. Li, *ACS Nano*, 2009, **4**, 380-386.
14. R. Leary and A. Westwood, *Carbon*, 2011, **49**, 741-772.
15. A. Fujishima and K. Honda, *Nature*, 1972, **238**, 37-38.
16. T. K. Townsend, N. D. Browning and F. E. Osterloh, *ACS Nano*, 2012, **6**, 7420-7426.
17. M. Kazuhiko, *Journal of Photochemistry and Photobiology C: Photochemistry Reviews*, 2011, **12**, 237-268.
18. X.-Y. Zhang, H.-P. Li, X.-L. Cui and Y. Lin, *Journal of Materials Chemistry*, 2010, **20**, 2801-2806.
19. P. Cheng, Z. Yang, H. Wang, W. Cheng, M. Chen, W. Shangguan and G. Ding, *International Journal of Hydrogen Energy*, 2012, **37**, 2224-2230.
20. Y. K. Kim and H. Park, *Energy & Environmental Science*, 2011, **4**, 685-694.
21. A. Suryawanshi, P. Dhanasekaran, D. Mhamane, S. Kelkar, S. Patil, N. Gupta and S. Ogale, *International Journal of Hydrogen Energy*, 2012, **37**, 9584-9589.
22. A. Mukherji, B. Seger, G. Q. Lu and L. Wang, *ACS Nano*, 2011, **5**, 3483-3492.
23. N. Li, G. Liu, C. Zhen, F. Li, L. Zhang and H.-M. Cheng, *Advanced Functional Materials*, 2011, **21**, 1717-1722.
24. J. Yu, B. Yang and B. Cheng, *Nanoscale*, 2012, **4**, 2670-2677.
25. W.-J. Chun, A. Ishikawa, H. Fujisawa, T. Takata, J. N. Kondo, M. Hara, M. Kawai, Y. Matsumoto and K. Domen, *The Journal of Physical Chemistry B*, 2003, **107**, 1798-1803.
26. *R. Abe*, *T. Takata*, *H. Sugihara* and *K. Domen*, *Chemical Communications*, 2005, 3829-3831.
27. L. M. Torres-Martínez, R. Gómez, O. Vázquez-Cuchillo, I. Juárez-Ramírez, A. Cruz-López and F. J. Alejandre-Sandoval, *Catalysis Communications*, 2010, **12**, 268-272.
28. H. Husin, H.-M. Chen, W.-N. Su, C.-J. Pan, W.-T. Chuang, H.-S. Sheu and B.-J. Hwang, *Applied Catalysis B: Environmental*, 2011, **102**, 343-351.
29. B. Zielińska, E. Mijowska and R. J. Kalenczuk, *Materials Characterization*, 2012, **68**, 71-76.
30. G. Hitoki, T. Takata, J. N. Kondo, M. Hara, H. Kobayashi and K. Domen, *Chemical Communications*, 2002, 1698-1699.
31. M. Hara, G. Hitoki, T. Takata, J. N. Kondo, H. Kobayashi and K. Domen, *Catalysis Today*, 2003, **78**, 555-560.
32. G. Hitoki, A. Ishikawa, T. Takata, J. N. Kondo, M. Hara and K. Domen, *ChemInform*, 2002, **33**, 7-7.
33. C. Singh, M. S. P. Shaffer and A. H. Windle, *Carbon*, 2003, **41**, 359-368.
34. W. S. Hummers and R. E. Offeman, *Journal of the American Chemical Society*, 1958, **80**, 1339-1339.
35. Y. Zhu, F. Yu, Y. Man, Q. Tian, Y. He and N. Wu, *Journal of Solid State Chemistry*, 2005, **178**, 224-229.
36. D. Eder and A. H. Windle, *Advanced Materials*, 2008, **20**, 1787-1793.
37. D. J. Cooke, D. Eder and J. A. Elliott, *The Journal of Physical Chemistry C*, 2010, **114**, 2462-2470.
38. J. Yu, L. Qi and M. Jaroniec, *The Journal of Physical Chemistry C*, 2010, **114**, 13118-13125.
39. D. Eder and A. H. Windle, *Journal of Materials Chemistry*, 2008, **18**, 2036-2043.
40. T. Takata, K. Shinohara, A. Tanaka, M. Hara, J. N. Kondo and K. Domen, *Journal of Photochemistry and Photobiology A: Chemistry*, 1997, **106**, 45-49.
41. H. Kato and A. Kudo, *The Journal of Physical Chemistry B*, 2001, **105**, 4285-4292.
42. S. Ikeda, A. Tanaka, K. Shinohara, M. Hara, J. N. Kondo, K.-i. Maruya and K. Domen, *Microporous Materials*, 1997, **9**, 253-258.
43. A. Kudo, H. Kato and S. Nakagawa, *The Journal of Physical Chemistry B*, 1999, **104**, 571-575.
44. S. Aksel and D. Eder, *Journal of Materials Chemistry*, 2010, **20**, 9149-9154.
45. H.-C. Huang and T.-E. Hsieh, *Journal of Applied Polymer Science*, 2010, **117**, 1252-1259.
46. M. Çelikbilek, A. E. Ersundu and S. Aydın, in *Advances in Crystallization Processes*, ed. D. Y. Mastai, InTech, 2012.

